Designing and Testing a CubeSat Bus with High-Thrust High-DeltaV Propulsion Capabilities

Faris Hamdi[1] and Kenneth Benedictos[2],
University of California, San Diego, La Jolla, CA, 92093

Christopher Ellis[3],
University of California, San Diego, La Jolla, CA, 92093

and

Ester Park[4]
University of California, San Diego, La Jolla, CA, 92093

The SEDS UCSD (Students for the Exploration and Development of Space Chapter at the University of California, San Diego) CubeSat bus design is presented below. The purpose of this CubeSat bus design is to improve upon the capabilities of cubesats by utilizing advanced technologies like additive manufacturing, and powerful modern processors. The incorporation of high delta-V capabilities, additional power, volume and mass budgets allows for the integration of all manner of payloads into mission profiles conventional cubesats are incapable of performing. The current design is in the testing phase, and the testing results along with the analysis and simulation data will be presented.

Nomenclature:

C&DH = Command and Data Handling.
DMLS = Direct Metal Laser Sintering (3-D printing) fabrication
Data block = 1024 bits of random data generated by a NASA-provided algorithm as prescribed by NASA
EM-1 = Exploration Mission 1
GNC = Guidance, Navigation and Control
H2O2 = Hydrogen Peroxide
ICPS = Interim Cryogenic Propulsion Stage
NASA MSFC = NASA Marshall Space Flight Center
Operating Period = continuous 30-minute time segment
SEDS UCSD = Students for the exploration and development of space
SLS = Space Launch System

I. Introduction

Designs for conventionally larger satellites have necessarily demanded, on average, \$10-100 million to fabricate, so in lieu of their increasing costs and scales of development, CubeSats have generated much attention by NASA. CubeSats, by contrast to their conventional, larger satellite counterparts, exhibit an extraordinary advantage over space exploration due to its significant reduction in mass, power, development time and cost. Specifically,

---

[1] Undergraduate Student, Department of Mechanical and Aerospace Engineering, AIAA Student Member
[2] Undergraduate Student, Department of Mechanical and Aerospace Engineering, AIAA Student Member
[3] Undergraduate Student, Department of Electrical and Computer Engineering
[4] Undergraduate Student, NanoEngineering Department

NASA has declared a second Centennial Cube Quest Challenge in order to expand research of these nanosatellites, and different approaches must be considered in order to maintain the highest caliber of efficiency. Therefore, Students for the Exploration and Development of Space at the University of California, San Diego (SEDS UCSD) will be approaching this challenge by building Triteia: a 6U configuration CubeSat designed to achieve a polar lunar orbit from a trans-lunar injection trajectory through the SLS EM-1 secondary payload deployment sequence. By utilizing additively manufactured propulsion unit, Triteia transforms from an unassuming, ordinary CubeSat to, instead, an autonomously intelligent power management system with a state-of-the-art additively manufactured high test H_2O_2 hydrogen peroxide propulsion unit. This is an unprecedented level of detail in design as Triteia's propulsion system utilizes a high test H_2O_2 thruster, which allows for extraordinarily faster in-space translational speeds, and it includes direct metal laser sintering (DMLS) techniques that manufacture the thruster into 3 separate sections: the diffuser plate, reaction chamber, and the nozzle. The Triteia cubesat bus will be explored in the context of the lunar orbit environment and the NASA CubeQuest mission profile.

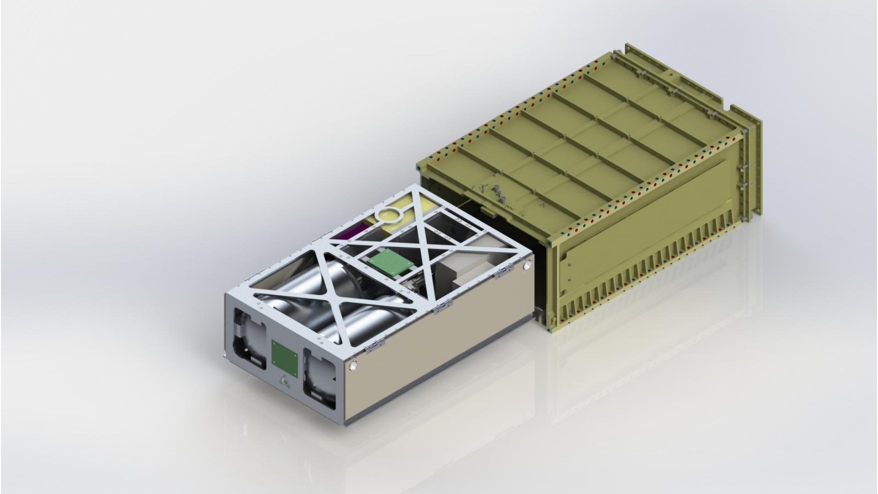

Figure 1-1: Rendered image of the Triteia Cubesat in its 6U planetary systems deployer.

As the first undergraduate student organization in the world to have successfully fabricated a full-size, additively manufactured, liquid-fueled rocket thruster, SEDS UCSD has patented two additively manufactured engines to date: the Vulcan-1 and the Tri-D. With funding from NASA MSFC, both rocket thrusters have been tested using an in-house fabricated static fire system, and experimental results have been published accordingly. Nonetheless, for this Ground Tournament-2, SEDS UCSD will embark on designing an entirely new, Hydrogen Peroxide (H_2O_2) monopropellant propulsion system with never-before seen delta v and thrust capabilities onto the 6U Triteia CubeSat. Upon anticipation for securing the Lunar Derby prize, this sophisticated propellant structure will be the first of its kind to evolve away from the conventional electric propulsion thrusters.

Mission objectives:

Primary

Under the conditions outlined by the Lunar Derby challenge, Triteia's primary mission objective consists of winning all 3 remaining Ground Tournaments (including the current GT-2) in order to secure an acceptance into the

SLS EM-1 secondary payload deployment. With sequence of precedence, the “Lunar Propulsion” in-space prize will be achieved by reaching one verifiable Lunar Orbit and maintaining the greatest communication distance, made possible from its unique chemical propulsion system. The in-space prize for “Spacecraft Longevity Contest” will be achieved by maintaining the longest elapsed number of competition days between the first and last confirmed reception with error-free, 1024-bit data block; furthermore, undaunted by Triteia’s robust radiation tolerant modules, autonomous power systems and mechanical controls, the active/passive actuated navigation commands will be transceivable through a real-time processor during flight sequence, thereby mitigating faults and inefficiencies altogether for highest spacecraft longevity.

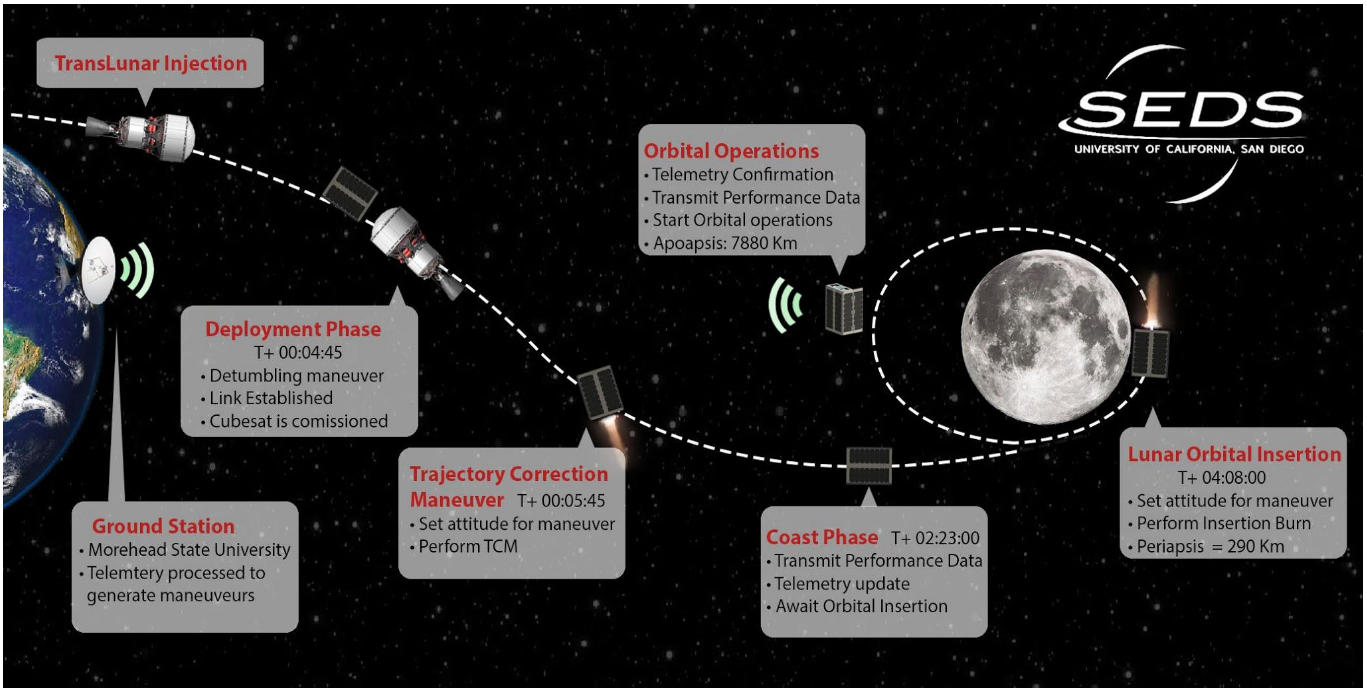

Figure 2-1: Triteia concept of operations and mission timeline

Secondary

Triteia will also perform in-space experiments and demonstrations that will actively advance the capabilities needed to take humans farther into space. The roadmap for secondary mission objectives of Triteia includes analyzing real-time thruster performance data from its monopropellant engine and reconciling it with measured calculations for future additively manufactured thruster actuation publication. New propulsion control algorithms will be demonstrated through sensor value responses obtained from its engine performance data, such as changing temperatures and varying pressures, and how they correspond to environmental perturbation. With regards to its electrical control algorithms, Triteia’s power systems architecture will be running a series of experiments for its optimization mechanism between communication rates, power input, and thermal state in order to maximize aggregated wattage efficiency across all power sinks. Triteia will also perform an array of experiments that test new technologies pertaining to advanced radio-frequency communication relays, navigation signals/processing and attitude control determination methods. Further experiments of attitude determination and control subsystem (ADCS) algorithms for Triteia will be performed through its mechanical systems architecture, with the intention of evolving its autonomous pre-programmed logic into a fully-fledged intelligent ADCS system. Later experiments will be conducted to validate the mode-results of the ADCS operation of Triteia and the transformation between the modes will also be individually studied thereafter.

II. System Design

The Triteia CubeSat consists of 7 main subsystems: Communication, Command and Data Handling (C&DH), Chassis, Power Systems, Propulsion, Guidance Navigation and Control, as well as Thermal Management. The main driving system requirement is to achieve lunar orbit, while advancing the state of propulsion by using additive manufacturing and verifying communication capabilities with the goal of maintaining operational power and thermal states. The system is designed accordingly, with precedence set for the propulsion system.

The Power Systems and the C&DH subsystems were designed for reliability and are mainly defined by the on-board software dictating the function states. This allows Triteia operational flexibility in case of anomalies or partial system failures. As the mission objective is to maintain a high system reliability, robust and fault tolerant components were chosen to uphold system functionality in case of sub-system failure. Both subsystems are built upon radiation tolerant processors and electronics with flight heritage to maintain reliability.

Thermal Control of the system shall be mainly passive. However, to provide increase the number of sustainable attitude modes the system shall utilize the attitude determination and control system to adjust the solar radiation input into the system. This shall be accomplished by varying the surface area exposed to sunlight, and powering down heat generating components. Furthermore, Thermal control shall algorithms shall interact with power generation and communication link algorithms to identify the most efficient attitude possible that provides the maximum communication window, while maintaining an optimum thermal state and sufficient power input.

On the ground operations side, the system will consist of a ground station, mission control and a development center. The ground station will be at moore state university which includes a 21m dish antennae. Mission control, on the other hand, will be located at the University of California, San Diego, and will contain flight and mission planning software to plot maneuvers during the mission. Additionally, mission control will serve to issue commands and telemetry to the CubeSat during mission operations. The development center will consist of a ground prototype, data analysis software, and appropriate testing environments to develop more efficient software iterations.

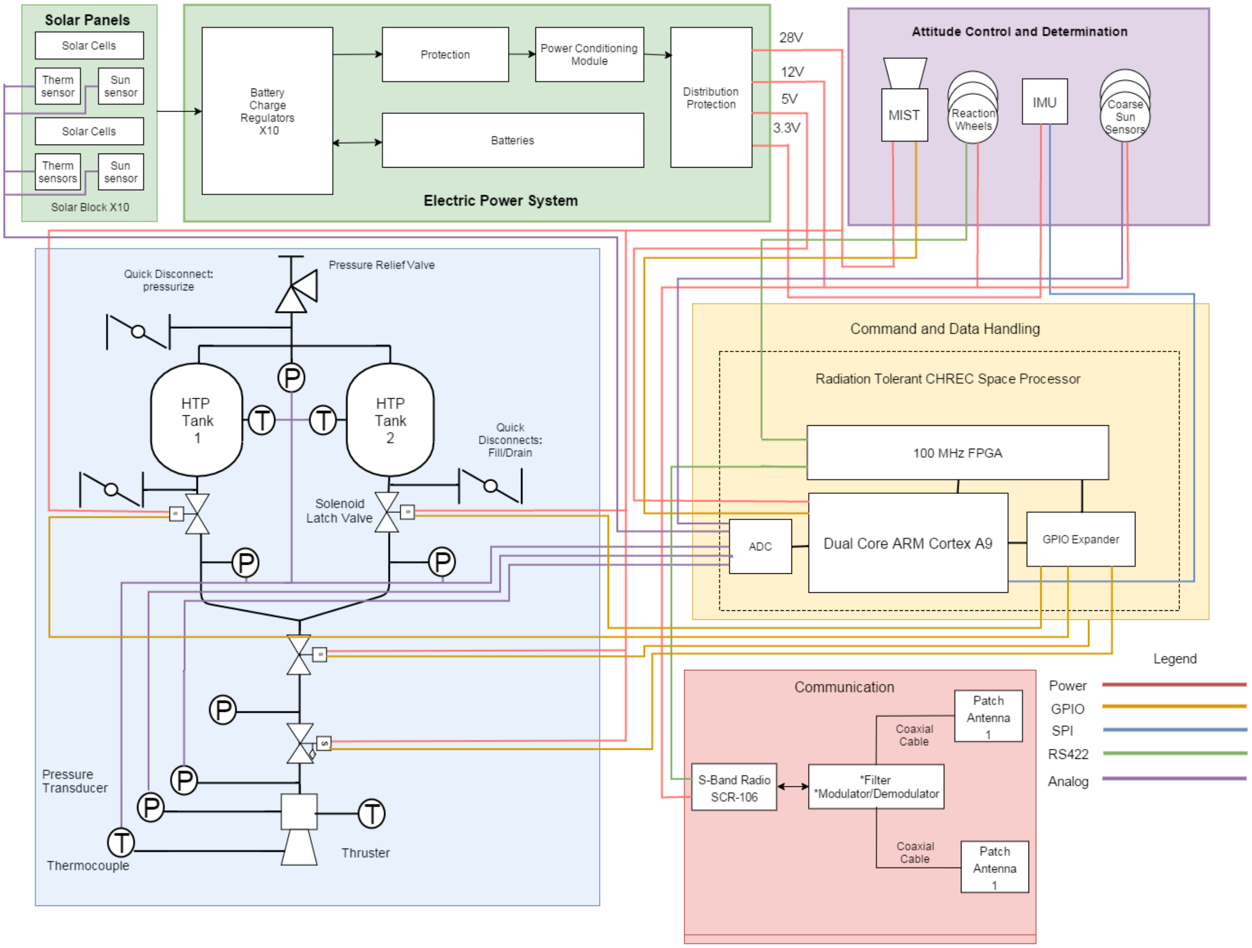

Figure 4-1: Triteia Systems Block diagram depicting the various interfaces between subsystems

III. Sub-Systems

The descriptions for the multiple subsystems are described and laid out in this section. The sub-systems introduced are propulsion, command and data handling, chassis, power system, guidance, navigation and control (GNC), communication, and ground station.

Propulsion

The propulsion system utilizes an additively manufactured 1 lbf thruster using 90% concentration H_2O_2 as the propellant through a blowdown system with dual tanks. The printing process uses direct metal laser sintering (DMLS) techniques to manufacture the thruster in 3 separate sections: the diffuser plate, reaction chamber, and the nozzle. Only the catalyst package, that will be housed in the reaction chamber, will need to be put together separately; subsequently, the engine will be assembled by bolting the flanges on each printed section together. The printed sections of the thruster will consist of inconel 718, whereas the catalyst package will be made up of silver and nickel screens, also with inconel 718 anti-channel baffles. The full length of the engine from inlet to nozzle will span 3.46 inches with the maximum diameter at the flanges being 1.64 inches and 0.32 inches in diameter along the reaction chamber. With a specific impulse of 155 seconds, the delta-V is 464 m/s.

Currently, the thruster has been sent to Metal Technology Industries where it is being printed. Once the engine is delivered, the catalyst package will be fabricated along with the static firing testing system. It is projected to be complete and cold flow tested by late March. After multiple “hot” fire tests, analysis, and iterative changes with this engine throughout the months of April and May, the design and fabrication of an engineering model of the cubesat propellant feed system is expected to be complete by early June. Soon after, the engineering model of the engine will be finalized, printed and tested to confirm the most optimal design. These tasks shall be completed by Ground Tournament 3 with system integration being the main focus of Ground Tournament 4.

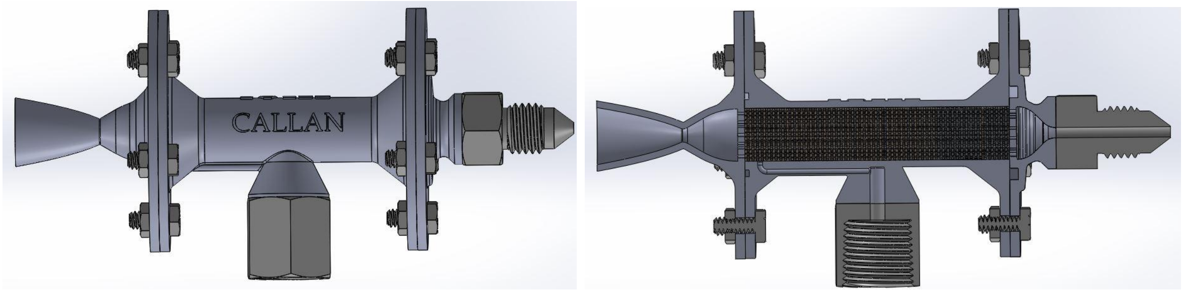

(a) **(b)**

Figure 4-2: (a) CAD model side view of the Callan monopropellant thruster. (b) CAD model side view cross section of the Callan monopropellant thruster.

Delta-V Budget

The maneuvers will play a crucial role in transitioning the spacecraft between different mission phases. Due to the constraints on the allowed mass and dimensions of the spacecraft, it is imperative that these maneuvers be as efficient as possible in order to minimize the overall mass of propellant required. With a specific impulse of 155 seconds, the total delta-v is calculated to be 452.8 m/s.

There will be two major maneuvers necessary from cubesat deployment to propel Triteia into Lunar orbit. The first is a trajectory correction to be performed as soon as possible upon deployment from the ICPS, once detumbling is complete and a communication link has been established. This maneuver ensures that the spacecraft will be oriented to enter a polar orbit upon arrival at the moon. It was minimized under the constraints that the spacecraft's final orbit must remain stable for at least 365 days and it's inclination must remain between 85° and 95°. The second maneuver is performed at periapsis in the retrograde velocity direction. This burn will take the spacecraft off of it's hyperbolic approach trajectory and onto an elliptic capture orbit. It was minimized under the constraint that the defines a lunar orbit as having a perilune greater than 300 km and an apolune less than 10,000 km.

The following table summarizes the Delta-V allocation for each maneuver in the mission, as well as the additional budget in case of misfires or other emergencies. All velocities are in meters per second.

Table 4-1: Overview of Delta-V budget

Mission Phase	**Maneuver Name**	**Delta-V (m/s)**	**Notes**
Cruise	Trajectory Correction Maneuver (TCM)	46	
Orbit Insertion	Lunar Orbit Injection (LOI)	350	
	Margin	56.8	To be used for additional correction maneuvers, the

			protection of historic lunar sites, etc.
		452.8	Grand total delta-v for mission

Command & Data Handling

C&DH utilizes Space Micro's Radiation Tolerant CHREC Space Processor in order to process data gathered from the CubeSat's sensors and any data that is uplinked to the CubeSat from the ground station. This data will be used to determine elements such as system health and the CubeSat's attitude. These elements will be used to determine what commands need to be scheduled and executed. The types of commands being scheduled will depend on the mode that the CubeSat is operating in. The modes are based on the timeline of the mission and the health of the system. There will be different modes representing stages of mission until the CubeSat performs a trans-lunar injection. After trans-lunar injection has occurred, the CubeSat will maintain a lunar orbit while switching between a mode that will focus on generating power and a mode that will focus on communication. If the CubeSat has any problems during the mission, then it will enter a contingency mode try to resolve the problem.

Chassis

The chassis, fabricated from two aluminum 7075-T6 blocks, shall serve to house all of the CubeSat internal components during storage, launch and in space. Specifically, the chassis shall be able to withstand launch stresses, shocks and vibrations. The chassis is designed with the highest strength to weight ratio in mind, and hence the material choice. The ease of fabrication and cost were also factors in the choice of material and fabrication method. The structure also houses two deployable solar panels and contains a spring-loaded nichrome wire triggered deployment mechanism. The current chassis is fabricated in two pieces to minimize structural interfaces and maintain strength. Multiple chassis will be built for testing and qualification purposes.

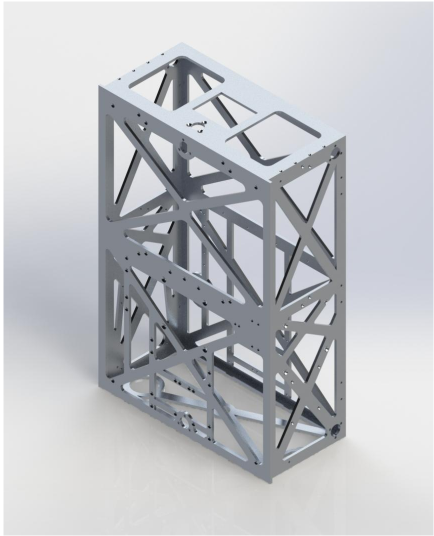

Figure 4-3: Isometric view of chassis CAD model without components or attachments

Space Craft Configuration

The Spacecraft is segmented between the propulsion unit and the other subsystems. A major driving factor was the mass distribution of the components in order to keep the center of mass in line with the thruster and keep the reaction wheels working at an efficient angle to avoid maximum power draw and tumbling. In addition, the mass has to be kept to a minimum for Tritea to require the least amount of fuel for volume sake.Wiring for interfacing and power between various electronic components requires proximity.

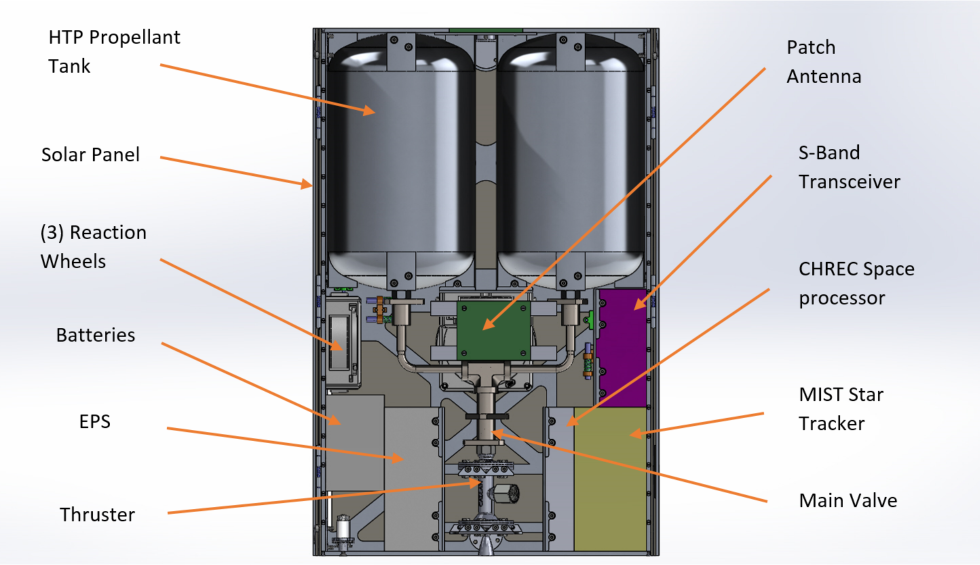

Figure 4-4: Configuration diagram illustrating the placement of major components and their mounts

Volume and Mass Budget

Table 4-2: Volume and parameter budgets

Major Components					
Teams	**Part name**	**Quantity**	**Box Dimensions (mm)**	**Total Volume (mm^3)**	**Total Mass (g)**
Astrodynamics	None	0	0	0	0
Chassis and Attitude Control	Chassis	1	n/a	331533	1057
	Reaction Wheels (RWp100)	3	70 x 70 x 25	367500	1050
	Mounting Equipment	4	100 x 100 x 1.5	60000	150
Communications	S-Band Transceiver (SCR-100)	1	82 x 82 x 35	235340	290
	Patch Antenna	2	50.89 x 41.18 x 3.1	12993	30
Power and Charging	Battery enclosure	1	77.3 x 40.7 x 66.7	209846	85
	Batteries	8	73.2 x 36.6 x 63.1	included above	388
	Electrical Power System	1	100 x 100 x 40	400000	300

	6 Unit Face Solar Panel	1	213.1 x 366 x 1.5	116992	290
	3 Unit Face Solar Panel	4	94.7 x 366 x 1.5	207961	540
Avionics & Attitude Determination	Radiation Tolerant CHREC Space Processor	1	100x100x30	300000	200
	SpaceMicro Miniature Integrated Star Tracker (MIST)	1	100 x 100 x 50	500000	500
	SpaceMicro CSS-01,02 Coarse Sun Sensors	3	22.86 x 22.86 x 8.99	14094	30
Propulsion	Engine	1	2.974 x 2.974 x 11.63	90773	83
	Valves	4	16 x 16 x 36	36864	96
	Propellant Tank	2	178.9 x 102.8 x 102.8	3784962	350
	H202 Propellant	n/a	178.9 x 102.8 x 102.8	included above	2272
Etc.	Smaller components (insulation, wires, etc.)	n/a	n/a	n/a	125
Total				6668858	7836
Safety Margin of 16.5%				8336072	9128
Maximum Available				10146984	14000
Extra Available				3478126	164
Percentage Used				82	65

Power System

The power system consists of solar panels, batteries, voltage converters, and circuit protection. Design considerations included power draw, voltage requirements, the orbit type, attitude requirements, mass, volume, and thermal limits. Care has to be taken in isolating failures to continue operating even under functional limitations. In order to ensure a reliable system, parts with strong heritage were implemented when possible and other cubesat designs were consulted to identify potential failure points. Each subsection of our system will ultimately contain space and radiation hardened parts. These will operate in accordance to the needs of the mission

The general power flow beginning with solar energy harvesting and ending in payload power supply is documented below in out top level system diagram. Larger arrows indicate power/energy flow and smaller arrows around the distribution section indicate the direction that our protection schemes will be operating in.

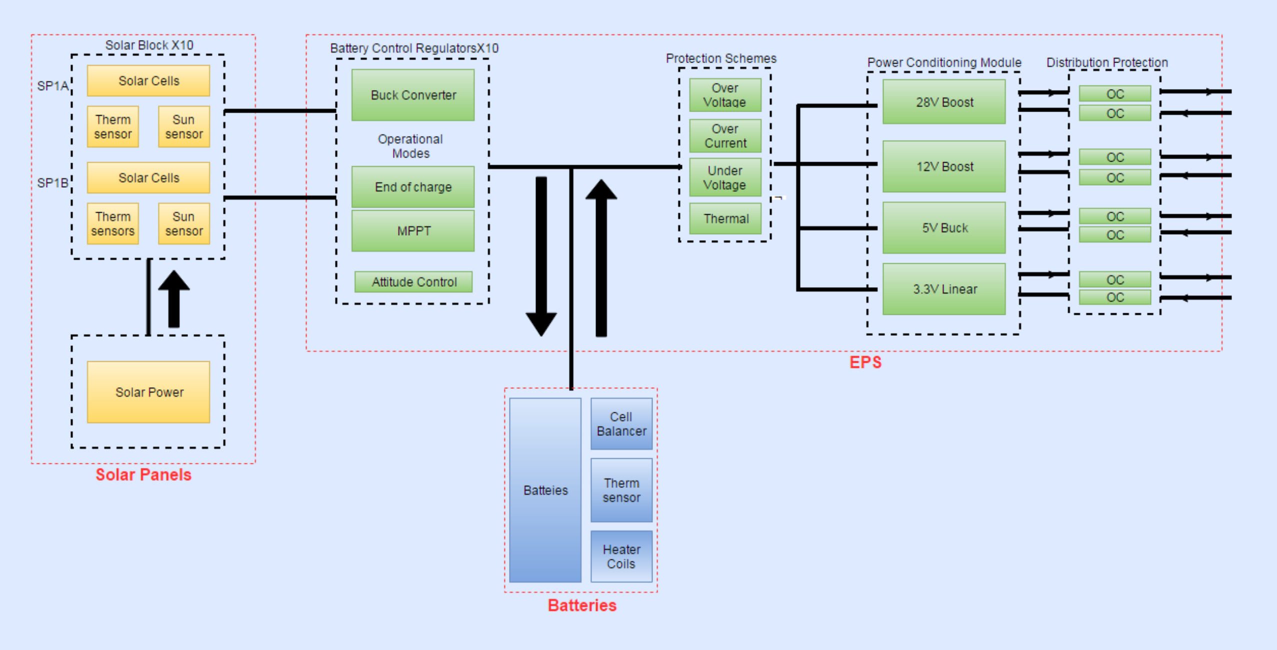

Figure 4-5: Power System top level block diagram

Power Budget

Power system assumptions:

- It is assumed that the EPS is 70% efficient from battery to payload
- It is assumed that the reaction wheels will be 30% saturated after LOI
- Is it assumed that there is no quantifiable power generation from solar panels during maneuvers, communications, and propulsion burns

Table 4-3: Power Budget (Deployment to Completion of two Orbits)

State	Solar (W)	Battery (Whr)	Avg Load (W)	Max Load (W)	Time (hr)
Deployment	-	91.76	5.72	5.72	0.0167
ACM	-	86.9	48.67	48.67	0.1
CM	-	76.9	20.02	20.02	0.5
ACM	-	72	48.67	48.67	0.1
TCM	-	71.6	15	47.2	0.025
ACM	-	66.73	48.67	48.67	0.1
Coast	22.6	91.76	12.2	12.2	40
ACM	-	86.9	48.67	48.67	0.1
CM	-	53.9	26.5	26.5	1
ACM	-	49	48.67	48.67	0.1
Coast	22.6	91.76	12.2	12.2	60
ACM	-	86.9	48.67	48.67	0.1
LOI	-	81.5	21.5	47.2	0.25
ACM	-	76.6	48.67	48.67	0.1
CM	-	43.6	33	63	1
ACM	-	38.7	48.67	48.67	0.1
Orbit	32	91.76	18.6	18.6	20.75

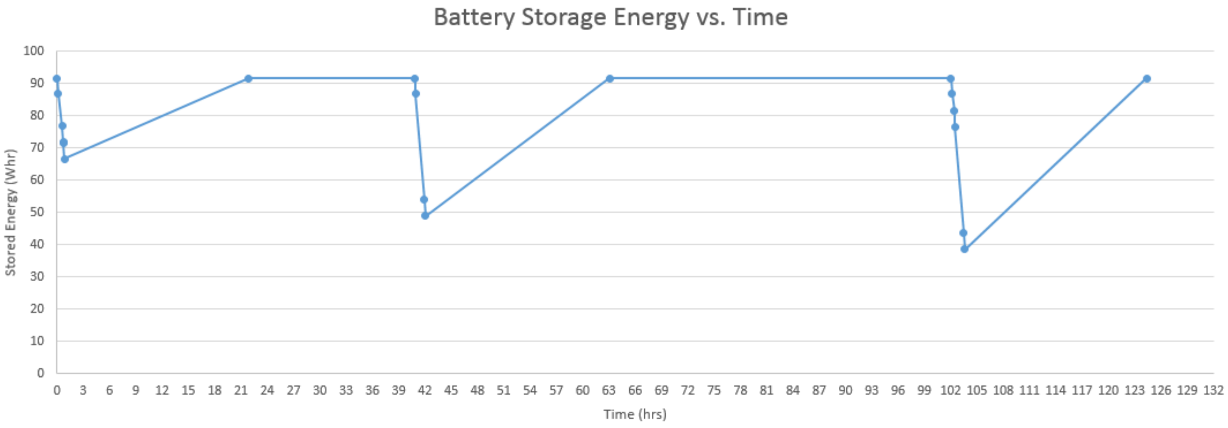

Figure 4-6: Battery Storage vs Time (Deployment to Completion of two Orbits)

4.1.4.2. Electrical Power System (EPS) Requirements

The EPS needs to efficiently and reliably provide power to all of the electrical loads of the cube satellite. The EPS should have an efficiency no less than 70% when transferring power from the Solar Panels to the payloads as well as from the batteries to the individual payloads. The major points of losses include switches, converters, and control support circuits.

The EPS needs to be able to support a minimum voltage of 10V and maximum voltage of 25V from the solar panels. The EPS needs to accommodate up to 1A per solar panel circuit.

The EPS needs to be robust enough to offer a wide variety of voltages to accommodate common voltages found on COTS parts and modules made specifically for cube satellite applications. The voltages that need to be present on the EPS are: 3.3V, 5V, 12V, and 28V

The EPS needs to have protection against overcurrents on the loads as well as overvoltage and undervoltage protection on the battery rail. The overvoltage and undervoltage protection needs to restrict the battery voltage to no more than 4.2V per cell and no less than 3.2V per cell.

The EPS needs to be able to accommodate the loads listed below:

Table 4-4: Payload Power Usage

	Max Power (W)	**Voltage (V)**	**Max Current (A)**
MIST	3.0	28.0	0.107
Valves (x4)	8.0	28.0	0.286
Transceiver	10.0	12.0	0.833
Reaction Wheels (x3)	9.0	12.0	0.750
CPU	4.0	5.0	0.800
Gyroscope	0.033	3.3	0.010

4.1.6. Communication

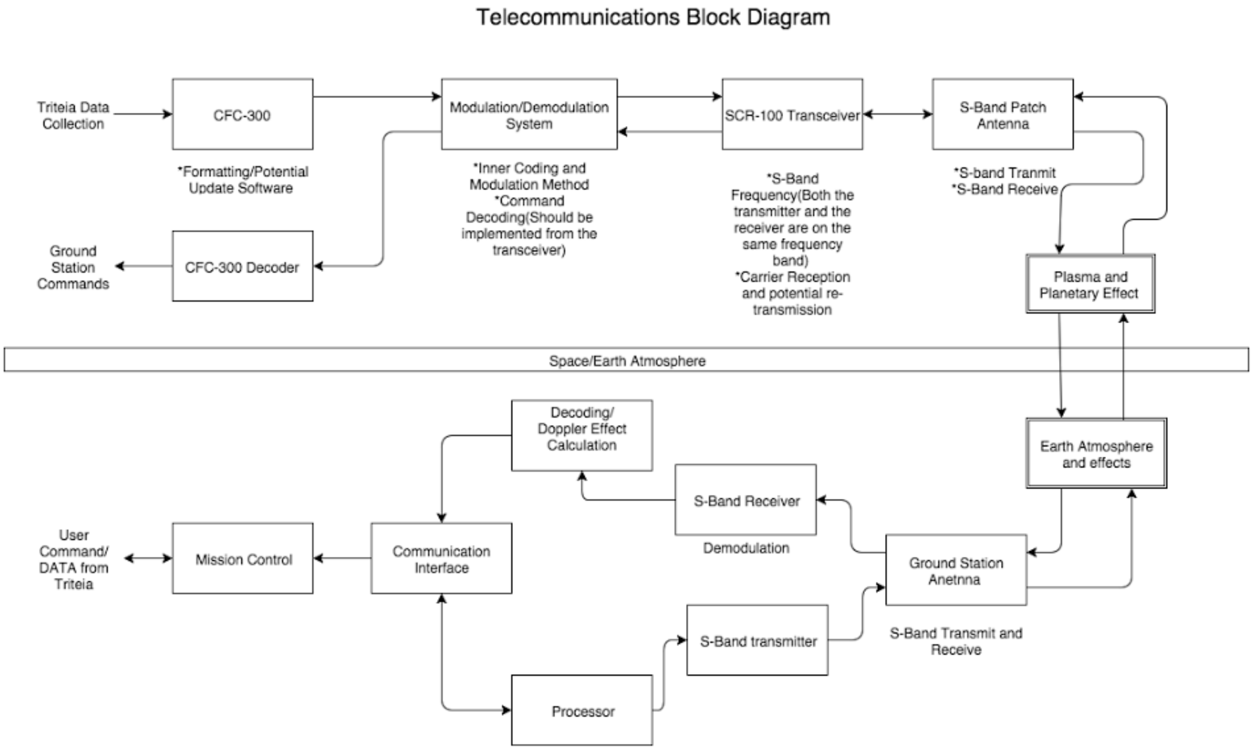

Figure: 4-11: The Telecommunications Block Diagram path is presented.

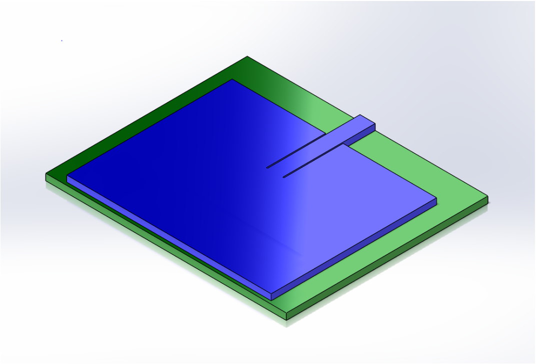

Figure 4-12: Block diagram illustrating the flow of uplink and downlink information between the Triteia Spacecraft and the Morehead State University 21m Antenna

The communication system will consist of one subsystem containing a transceiver and two patch antennas. Radio commands and telemetry will be processed by Innoflight's SCR-100 transceiver located on the Triteia Spacecraft. The transceiver provides the data rate necessary for a stable margin in telecommunications. To maintain adequate communications, the transceiver will be receiving and transmitting information through two independent patch antennas. While dependent on Triteia's position in space, the patch antennas will be located on different sides of the Triteia in order to emit and receive at different angles. The transceiver will be managing all commands and modulation/demodulation processes on the communication system.

The two patch antennas will operate independently from one another. The time the patch antennas operate is dependent on the position of Triteia. Both of these patch antennas have an independent gain of 5.71 dBi and will be positioned on different sides of the Triteia spacecraft. The antennas will be approximately 50 mm by 41 mm and will both operate under S-band (2050-2250 MHz). The patch antenna will provide sufficient data rates in order to transmit images efficiently. The communication system will modulate and demodulate the transmitted signal and send the data to be processed by the CPU.

(Shown with optional diplexer/splitter)

Figure 4-13: 3-D Model of Rectangular Patch Antenna generated using Solidworks. Intended S-Band compact transceiver SCR-100 from Innoflight.

4.1.6.1 Link budget and Margin

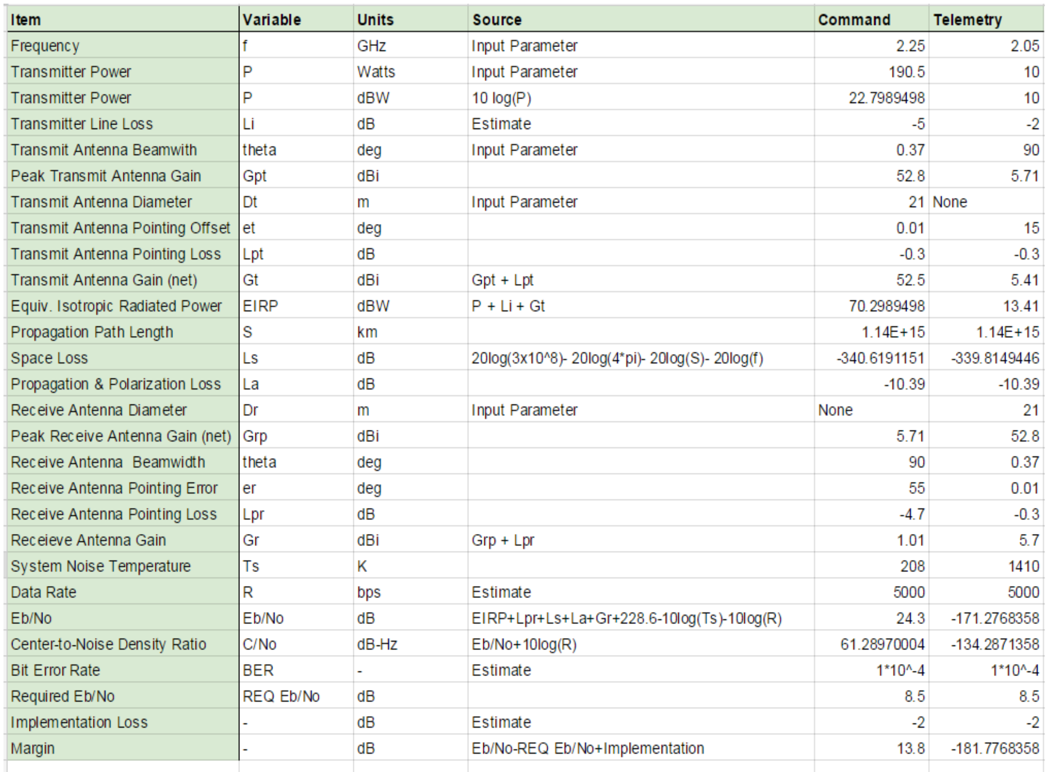

Item	Variable	Units	Source	Command	Telemetry
Frequency	f	GHz	Input Parameter	2.25	2.05
Transmitter Power	P	Watts	Input Parameter	190.5	10
Transmitter Power	P	dBW	10 log(P)	22.7989498	10
Transmitter Line Loss	Li	dB	Estimate	-5	-2
Transmit Antenna Beamwith	theta	deg	Input Parameter	0.37	90
Peak Transmit Antenna Gain	Gpt	dBi		52.8	5.71
Transmit Antenna Diameter	Dt	m	Input Parameter	21	None
Transmit Antenna Pointing Offset	et	deg		0.01	15
Transmit Antenna Pointing Loss	Lpt	dB		-0.3	-0.3
Transmit Antenna Gain (net)	Gt	dBi	Gpt + Lpt	52.5	5.41
Equiv. Isotropic Radiated Power	EIRP	dBW	P + Li + Gt	70.2989498	13.41
Propagation Path Length	S	km		1.14E+15	1.14E+15
Space Loss	Ls	dB	20log(3x10^8)- 20log(4*pi)- 20log(S)- 20log(f)	-340.6191151	-339.8149446
Propagation & Polarization Loss	La	dB		-10.39	-10.39
Receive Antenna Diameter	Dr	m	Input Parameter	None	21
Peak Receive Antenna Gain (net)	Grp	dBi		5.71	52.8
Receive Antenna Beamwidth	theta	deg		90	0.37
Receive Antenna Pointing Error	er	deg		55	0.01
Receive Antenna Pointing Loss	Lpr	dB		-4.7	-0.3
Receieve Antenna Gain	Gr	dBi	Grp + Lpr	1.01	5.7
System Noise Temperature	Ts	K		208	1410
Data Rate	R	bps	Estimate	5000	5000
Eb/No	Eb/No	dB	EIRP+Lpr+Ls+La+Gr+228.6-10log(Ts)-10log(R)	24.3	-171.2768358
Center-to-Noise Density Ratio	C/No	dB-Hz	Eb/No+10log(R)	61.28970004	-134.2871358
Bit Error Rate	BER	-	Estimate	1*10^-4	1*10^-4
Required Eb/No	REQ Eb/No	dB		8.5	8.5
Implementation Loss	-	dB	Estimate	-2	-2
Margin	-	dB	Eb/No-REQ Eb/No+Implementation	13.8	-181.7768358

Figure 4-14: Link Budget elaborates on the specifications of the Triteia Communications System, including estimated data rates and margin calculations.

The telecommunication system will be functioning at the S-Band and intends to utilize an uplink frequency of 2050 MHz and a downlink frequency of 2250 MHz. S-Band frequencies were chosen due to the system's low power budget and the need for a data rate capable of transmitting images to ground station. The ground station that was chosen and implemented in the system's calculations was the 21 meter antenna located and operated by Morehead State University in Ronald G. Eaglin Space Science Center (38° 11' 30.773 N, 83° 26' 19.948 W). The intended data rate for transmission is approximately 5000 bps.

Detailed specifications for the ground station are located in the ground station subsection and will provide transmission data found in the link budget. In regards to the telemetry modulation, the Triteia communication system will utilize BPSK (Binary Phase-Shift Keying) to modulate and demodulate transmissions. BPSK was chosen due to its low modulation rate and efficiency, both of which are important to the system. This decoding method will minimize the bit error rate in the system as well as increase the system's performance. Overall, the system will linked our system with a margin of approximately 13.8dB.

4.1.7 Ground Station

Figure 4-15: Visual of (left) Morehead State University 21m Antenna, (top right) Control Room, and (bottom right) Operation Center.

The Triteia Communication System plans to utilize the 21m Antenna at the Ronald G. Eaglin Space Science Center (38° 11’ 30.773 N, 83° 26’ 19.948 W), which is located and operated by Morehead State University. This system is a reliable choice as the Tritea ground station because of its capability of high gain and RF performance with the spacecraft. The ground station will be accessed through SSH (Secure Shell), which will allow the team to send commands to the CubeSat from the command center at the University of California, San Diego.

Testing and Additional Data

The paper will include more in depth thermal, vibration and stress analysis. In addition to system simulation data to verify both design and operation of the concept. Subsystem experimental data will also include Thruster Isp and thrust data, antenna radiation pattern and gain tests, as well as scenario analysis of LEO, GEO and Lunar missions and the payload compatibility of the bus.